Imine-coordinated 2-Aminoazole Complexes of Au(I): Complicating Reactions and Verification of Products by Crystal Structure Determination

Leigh-Anne de Jongh[a], Liliana Dobrzańska[a,b], Christoph E. Strasser[a], Helgard G. Raubenheimer[a], and Stephanie Cronje[a,c]

[a] Department of Chemistry and Polymer Science, University of Stellenbosch, Private Bag X1, Matieland, 7602, Stellenbosch, South Africa

[b] Department of Chemistry, Katholieke Universiteit Leuven, Celestijnenlaan 200F - bus 2404, B-3001 Heverlee, Belgium

[c] Institut für Anorganische und Analytische Chemie, Goethe-Universität Frankfurt, Max-von-Laue-Strasse 7, D-60348 Frankfurt am Main, Germany

Reprint requests to Dr. Stephanie Cronje. Fax: +27 (0)21 808-3849. E-mail: scron@sun.ac.za or stephanie.cronje@gmail.com

Z. Naturforsch. **2014**, *69b*, 1073 – 1087 / DOI: 10.5560/ZNB.2014-4187
Received August 11, 2014

Dedicated to Professor Hubert Schmidbaur on the occasion of his 80th birthday in recognition of his numerous important contributions to inorganic and organometallic chemistry

When Au(I) is provided with endocyclic soft thioether or endocyclic hard amine, endocyclic borderline imine and exocyclic hard amine coordination sites, the softer borderline endocyclic imine coordination site is favored. This is demonstrated by the synthesis and structural characterization (IR, MS, ^{1}H, ^{13}C and ^{31}P NMR experiments and single-crystal X-ray diffraction analysis) of 2-aminoazole (2-amino-4-methylthiazole, 2-aminobenzothiazole and 2-aminobenzimidazole) complexes of $[AuPPh_3]^+$ (**1**–**3**). An unusual ring opening is observed for the reaction of 2-aminothiazoline with $[Au(NO_3)PPh_3]$ yielding μ_2-(2-mercapto-ethyl-cyanamide-κ,S)bis(triphenylphosphine)gold(I) nitrate (**4**). Reactions of 2-aminoazoles with $Au(C_6F_5)$THT (THT = tetrahydrothiophene) yield $[Au(C_6F_5)_2]^-$ stabilized by various cations. The formation of Au(2-aminothiazoline)C_6F_5 is again the exception.

Key words: Au(I), 2-Aminoazole, 5-Membered Heterocycle, Homoleptic Rearrangement, Aurophilic Interactions, Sulfonium Complex

Introduction

Many biomolecules such as proteins, enzymes, nucleic acids and some vitamins which are essential to life processes contain five-membered azoles (excluding oxazoles) and their derivatives which are important units in the basic structure of these molecules [1, 2]. Numerous metal ions have a crucial function in biochemical processes. Research in bioinorganic and bioorganometallic chemistry has been driven by the elucidation of the role of metal ions in enzyme function, as pharmaceuticals in diagnostics and therapy as well as toxicity studies [3 – 5]. The determination of the site of metallation of biomolecules is of great interest for the development of metallopharmaceuticals, characterization methods in molecular biology as well as for the immobilization of biomolecules on metal surfaces [6]. The anti-proliferative, *i. e.* antiviral, anti-bacterial, anti-fungal, anti-microbial, anticancer, anti-inflammatory, and anti-infective activity of gold(I) compounds and their clinical use in the treatment of severe rheumatoid arthritis have provided a powerful incentive for the continued pursuit of the bonding of biologically active molecules to gold(I) and the investigation of their biological effects [7 – 9]. The coordination of biologically active molecules to metal centers has afforded compounds with amplified activity or therapeutic effect [10].

The unexpected *N*-coordination of the enzyme cyclophilin to gold(I) *via* the nitrogen atom of an ac-

© 2014 Verlag der Zeitschrift für Naturforschung, Tübingen · http://znaturforsch.com

tive His residue, despite the presence of four Cys thiol groups, has implications for the understanding of the biochemical mechanisms of gold compounds [11]. The affinity of metal centers for exocyclic amine *versus* endocyclic imines or thioether coordination sites can be studied with simple but useful model compounds such as 2-aminoazoles. We have previously found that the endocyclic imine is the preferred coordination site of AuC_6F_5 units when provided with the former and exocyclic as well as endocyclic thioether coordination sites [12, 13]. Results have shown that the soft Au(I) acid center in a series of ligand substitutions, displays the following order in decreasing preference: C=S > R_2NH (hard base) ⋙ C=N– (borderline base) > RSR (soft base). This disagrees with the conventional classification of soft and hard acids and bases which indicates a decreasing preference C=S > RSR ≫ C=N– > R_2NH. It can be argued that the $C_6F_5^-$ ligand hardens the gold center, and it was necessary to also investigate the coordination site preference of the softer gold in $[AuPPh_3]^+$. Exocyclic imine coordination to gold is preferred by azol-2-ylideneamine ligands (azol-2-ylideneamine = 3,4-dimethyl-3*H*-thiazol-2-ylideneamine, 3-methyl-3*H*-benzothiazol-2-ylideneamine or 1,3-dimethyl-1,3-dihydro-benzimidazol-2-ylideneamine) in reactions with AuC_6F_5, $[AuPPh_3]^+$ or [Au(1,3-di-*tert*-butyl-imidazol-2-ylidene)]$^+$ units [14].

Coordination of borderline acids such as Co^{2+}, Zn^{2+} and Ni^{2+} to 2-aminoazole derivatives shows bonding to the endocyclic imine nitrogen [15]. $Cr(CO)_5$ and $W(CO)_5$ fragments, the former used as a protecting group in peptide synthesis and the latter as a label in biologically active molecules [16, 17], are of interest as soft Lewis acids. In the plethora of pentacarbonyl group 6 metal carbene compounds that have been reported, $W(CO)_5$ is a soft Lewis acid but upon coordination to 2-aminopyrimidine, a hard exocyclic sp^3 amine N is preferred [18, 19] even with an additional softer aromatic sp^2 imine N present, contradicting standard HSAB rules [18 – 20]. A sensitive balance has been struck between the coordination of $W(CO)_5$ units to exocyclic amino groups or to endocyclic imino groups in pyridines, pyrimidines and purines [19, 20]. When provided with endocyclic soft thioether or endocyclic hard amine, endocyclic borderline imine and exocyclic hard amine coordination sites present in 2-aminoazoles, the softer endocyclic imine coordination site is favored by both $Cr(CO)_5$ and $W(CO)_5$ units [21].

In the present study the metal centers $[AuPPh_3]^+$ and AuC_6F_5 were presented with several coordination sites present in various 2-aminoazole ligands, *i. e.* a soft endocyclic thioether, a hard exocyclic amine, a hard endocyclic amine and a softer borderline endocyclic imine. The characterization and structural elucidation of the isolated complexes, confirmed the preference of the gold center for the borderline endocyclic imine N unless complicating reactions such as ring opening of a saturated, substituted azole [22] with concurrent stabilization of the hypercoordinated phosphinogold(I) derivatives around an S center by Au···Au interactions [23], or homoleptic rearrangements [24] to yield $[Au(C_6F_5)_2]^-$ occur.

Results and Discussion

Synthesis

The treatment of equimolar amounts of the starting material $Au(NO_3)PPh_3$ [25] suspended in diethyl ether at room temperature with 2-amino-4-methylthiazole, 2-aminobenzothiazole, 2-aminobenzimidazole or 2-aminothiazoline dissolved in diethyl ether readily afforded complexes **1**–**4** (Scheme 1). After extraction of the obtained solids upon stripping of solvent (*in vacuo*) with diethyl ether, filtration and concentration, the products were obtained after trituration with pentane. The 'soft-borderline' adducts **1**–**3** and the dinuclear product, **4**, are neither air nor moisture sensitive. These cationic complexes are soluble in more polar organic solvents such as methanol, acetone and dichloromethane but insoluble in hexane and pentane.

Crystals suitable for X-ray diffraction for structure determinations were obtained from concentrated solutions of **1** (yellow) or **2** (yellow) in dichloromethane, **3** in methanol (**3b**, **3c**, colorless) or **4** in acetone (colorless) at −22 °C or by vapor diffusion of pentane into a solution of **3** (**3a**, colorless) under argon at −22 °C. Single-crystal structure analyses revealed that in **3a** the unit cell consists of a cation and anion only, while the unit cells of complexes **3b** and **3c** contain cations, anions and solvent molecules.

The crystals of **4** showed the formation of μ_2-(2-mercapto-ethyl-cyanamide-κ,*S*)bis(triphenylphosphine)gold(I) nitrate which reveals an interesting ring opening of the ligand, 2-aminothiazoline, *via* deprotonation of the amine, proton migration to the original imine and ring cleavage at the C–S

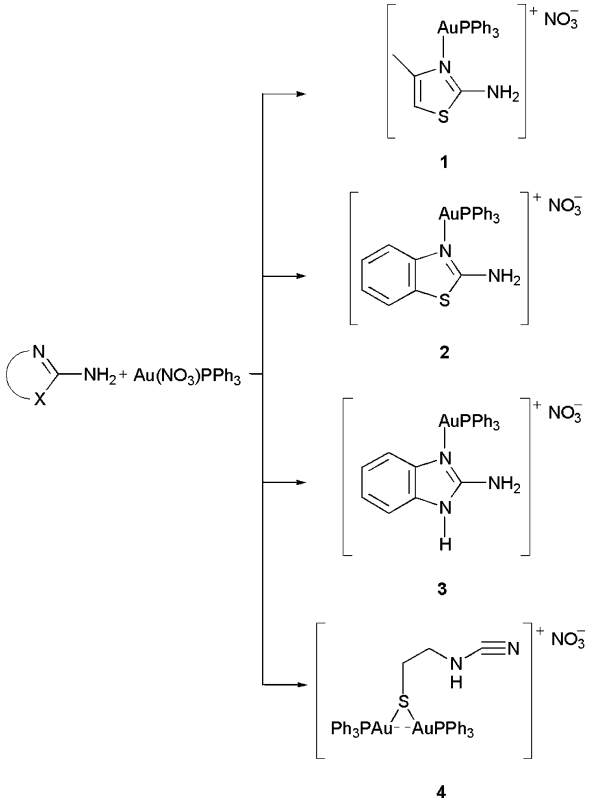

Scheme 1.

bond (not necessarily in this order). The concomitant coordination of two $[AuPPh_3]^+$ moieties in the product, μ_2-(2-mercapto-ethyl-cyanamide-κ,S)bis(triphenylphosphine)gold(I) nitrate, accentuates the important mediating influence of the cationic gold fragments. Notably, Laguna and co-workers observed a related ring opening [22] but by using $Au(acac)PPh_3$ as reactant effected a second deprotonation, amide coordination of one $[AuPPh_3]^+$ ion and the formation of a neutral product.

The most general route for the preparation of imine-functionalized heterocyclic (pentafluorophenyl)gold(I) compounds involves the substitution of the labile THT ligand in $Au(C_6F_5)THT$ by an imine ligand, yielding $Au(C_6F_5)L$ [12]. Such coordination was now only observed for **5** (an exception in the series). In all the other experiments a number of products that contain $Au(C_6F_5)_2^-$ anions and various aquated and/or ligated lithium or 2-aminoazolium cations were crystallized from the reaction mixtures (Scheme 2). Compound **5** was prepared by treating

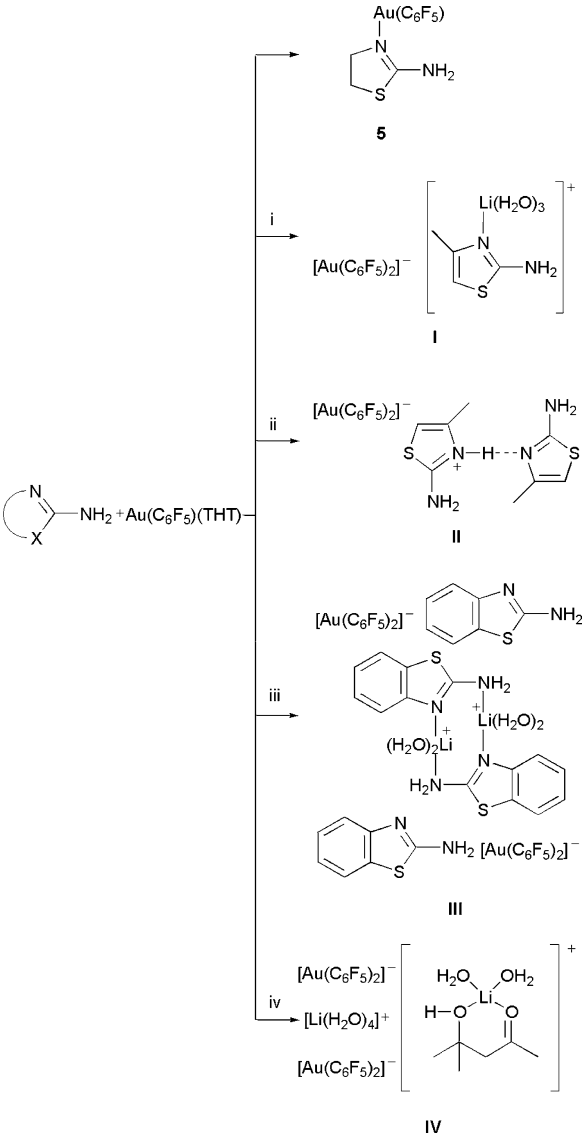

Scheme 2. i) 1.5 mol equivalents of 2-aminoazole, ii) 0.5 mol equivalents of 2-aminoazole, iii) 1.0 mol equivalent of 2-aminoazole, two crystallographically independent moieties present in the asymmetric unit of the crystals, iv) 1.0 mol equivalent of 2-aminobenzimidazole.

a solution of 2-aminothiazoline in diethyl ether with equimolar amounts of $Au(C_6F_5)THT$ at room temperature under inert conditions. From reaction mixtures prepared according to the same protocol with 2-amino-4-methylthiazole (using 1.5 or 0.5 mol equivalents of ligand), 2-aminobenzothiazole and 2-amino-1-methylbenzimidazole [21, 26] only crystals of prod-

ucts **I**–**IV**, resulting from homoleptic rearrangements and interactions of lithium cations with various ligands, were isolated and characterized by single-crystal structure determinations. Crystallizations were not performed under inert conditions. Lithium chloride, formed during the preparation of $Au(C_6F_5)THT$ [27] probably afforded the solvated or complexed lithium cations. The products discussed here are simply those that crystallized most readily. Product **III** is particularly interesting owing to the symmetric coordination of the lithium cations by two aminoazole ligands.

Such rearrangements with unpredictable incidence are common in gold(I) chemistry and not always reported. Examples are: i) the fragment of $[Li(diglyme)_{2.5}(ebtz)]^{+}_{\infty}$ and the non-interacting $Au(C_6F_5)^{-}$ which were obtained from the attempted synthesis of [1,2-di(tetrazol-2-yl)ethane](pentafluorophenyl)gold(I) by addition of 1,2-di(tetrazol-2-yl)ethane to 2 molar equivalents of $Au(C_6F_5)THT$; ii) the 2-dimethylamino(ethylene)-trimethylammonium cation ($TMRDAMe^{+}$) and non-interacting $Au(C_6F_5)_2{}^{-}$ formed from an attempted synthesis of (1-benzyl-4-methyltetrazol-5-ylidene)(pentafluorophenyl)gold(I) [28]; iii) the isolation of $[Au(C_6F_5)_2][Au(pdma)_2]$ [pdma = *o*-phenylenebis(dimethylarsine)] [29], and iv) the conversion of (isothiazol-5-yl)(pentafluorophenyl) gold(I) – see below [24].

While Raubenheimer and co-workers [24] have observed a homoleptic rearrangement for (isothiazol-5-yl)(pentafluorophenyl)gold(I), the complex (isothiazol-5-yl)(triphenylphosphine)gold(I) could be readily isolated. In the instance when isothiazole is used as *N*-heterocyclic ligand in the neutral complex (isothiazol-5-ylidene)(pentafluorophenyl)gold(I), the rearrangement occurs slowly and can be followed by ^{1}H NMR measurements. Trace amounts of the rearranged product formed within days, and the reaction reaches an equilibrium after 18 d. The reaction occurs more rapidly for the precursor (isothiazol-5-yl)(pentafluorophenyl)gold(I) and can be converted *in situ* into a carbene complex by immediate alkylation. In contrast, (triphenylphosphine)(isothiazol-5-yl)gold(I) is stable in solution and can readily be isolated in pure form. Subsequent alkylation of this product again affords a mixture that includes an ionic homoleptic rearrangement by-product.

Compound **5** is soluble in polar organic solvents such as acetone, dichloromethane and diethyl ether and insoluble in water and alkanes such as pentane and hexane. Crystals suitable for X-ray diffraction, were obtained from concentrated solutions of **5**, **I**, **II**, and **III** in dichloromethane or by vapor diffusion of pentane into a solution of **IV** in acetone.

Spectroscopic and spectrometric characterization

Most signals in the NMR spectra (^{1}H, ^{13}C, ^{31}P) of the new compounds appear slightly downfield to the chemical shifts of the corresponding starting materials. Although differences in concentration are known to influence the NH chemical shifts, it is notable that coordination to a gold(I) center has a varied, but pronounced effect on the NH_2 moiety of ligands. In most cases NH_2 resonances are shifted significantly downfield with respect to free ligand signals. This effect is more pronounced for complex **1** ($\delta = 1.76$ ppm) than for **2** ($\delta = 1.34$ ppm), along with increasing lone pair electron delocalization over the ligand system. In contrast, the NH_2 resonance of complex **3** experiences a significant upfield shift ($\delta =$ 3.02 ppm). Deshielding of the NH_2 protons in **3** by close association of the nitrate anion (even in solution), could give a plausible explanation for this divergence. Additionally, hydrogen bonds between oxygen atoms of the anion and NH_2 in the cation exist in the solid state of **3**. NMR studies and single-crystal structure determinations have illustrated a similar situation for the NH in (3,4-dimethyl-3*H*-thiazol-2-ylideneamine)$AuPPh_3$ [14], for the NC(H)N proton in $[\{\mu_2\text{-}HCCCH_2N{=}C(H)N(CH{=}CH_2)CH{=}CH\}Co_2(CO)_6][B(C_6H_5)_4]$ [30] and ferrocenyl imidazolium salts [31, 32]. Resonances for the NH group in **3** and its corresponding free ligand were not observed. The signal for the aliphatic amine in **4** ($\delta =$ 2.83 ppm) appears upfield from the signal for the primary amine in the starting material, 2-aminothiazoline ($\delta = 4.71$ ppm).

In the ^{1}H NMR spectra, resonances of the phenyl protons of benzazole-derived ligands ($\delta =$ 7.1 – 7.5 ppm) clearly show the chemical inequivalence of the phenyl C*CH* and CCH*CH* protons upon changing from an N atom in **3** (only two doublets of doublets detected) to an S atom (multiplets observed) in **2**. The signals indicating the presence of the $AuPPh_3$ moiety, appear as a multiplet in the same region ($\delta =$ 7.6 – 7.7 ppm) integrating for 15 (in the spectrum of **1**–**3**) or 30 H atoms (in the spectrum of **4**).

In the ^{13}C NMR spectra, the signal for the carbon atom situated between two heteroatoms is shifted downfield upon complexation in the thiazole (**1**, $\delta = 189.0$ ppm) and thiazoline/2-mercapto-ethyl-cyanamide (**4**, $\delta = 171.4$ ppm) compounds but upfield for the benzazole compounds **2** ($\delta = 142.1$ ppm) and **3** ($\delta = 156.9$ ppm). In the instance of the phenyl carbon atoms of the benzazole ligands some carbon atoms appear slightly downfield and others slightly upfield. This observation is not unusual as the total chemical shift s ($s = s_{\text{paramagnetic}} + s_{\text{diamagnetic}}$) in the ^{13}C NMR spectrum reflects more than simply shielding and deshielding as in the ^{1}H NMR spectrum [33]. In the spectra of **1 – 4**, four additional sets of doublets are detected in the region $\delta = 129 - 136$ ppm and correspond to the characteristic C–P coupling of the phenyl carbon atoms of the $[AuPPh_3]^+$ moiety. Of these, the doublet at $\delta = 129.0 - 130.4$ ppm can be assigned to the C–P-coupled *ipso*-carbon atom, whilst the doublet at $\delta = 131$ ppm is attributable to the C–P-coupled *meta*-carbon atom. Resonances of the *ortho*- and *para*-carbon atoms are observed as doublets in the regions $\delta = 134.5 - 136.3$ and 132.8 – 134.3 ppm, respectively.

In the ^{31}P NMR spectra only one intense singlet at $\delta = 30.6$ ppm for **1**, $\delta = 33.9$ ppm for **3** and $\delta = 37.1$ ppm for **4** is observed. These values appear somewhat downfield compared to the chemical shift in the precursor compound, $Au(NO_3)PPh_3$ ($\delta = 28.9$ ppm).

Compound **5** has been fully characterized previously by Laguna and co-workers [22] thus only its crystal structure is reported below. Small changes in chemical shift in the NMR spectra of **I**–**IV** made unambiguous characterization impossible. Although the C_6F_5 groups could for instance be observed, it was impossible to unequivocally determine whether the simple coordination compound or products of homoleptic rearrangement had formed. The spectra are thus neither reported nor discussed as single-crystal structure determinations had shown that in the instance of **5** the coordination product had formed but homoleptic rearrangements had yielded **I**–**IV**.

Solid-state ATR (attenuated total reflectance) FT-IR spectra were recorded for the ligands and complexes **1**–**4**. All spectra show very broad bands of weak intensity in the range $3054 - 3404\ cm^{-1}$, assignable to N–H stretching vibrations. The primary amine N–H stretches (asymmetric and symmetric) appear as 2 bands in the region $3385 - 3054\ cm^{-1}$ for **1**–**3** whereas a secondary amine N–H stretch is observed at $3295\ cm^{-1}$ for **4**. A smaller third band ($3054 - 3123\ cm^{-1}$) in the spectra of **1**–**3**, considered to be the result of interaction between an overtone of the N–H bending absorption band at $1627 - 1641\ cm^{-1}$ (also in-plane NH_2-scissoring) with the symmetric N–H stretching band, is also visible. Notably, N–H and C–N stretching bands ($1305 - 1312\ cm^{-1}$) of the complexes **1**–**3** are detected at lower wave lengths and the C=N stretching bands ($1531 - 1465\ cm^{-1}$) at higher wave lengths than in the free ligands suggesting electron delocalization over the carbon nitrogen bonds to be more pronounced in the coordinated ligands. In the IR spectrum of **4**, a C≡N stretching vibration at $2218\ cm^{-1}$ is clearly visible in addition to the N–H bending absorption at $1663\ cm^{-1}$, the C=N stretching ($1618\ cm^{-1}$) and the C–N aliphatic stretching vibration at $1310\ cm^{-1}$. The IR spectra of **I**–**IV** show the presence of 2-aminoazoles and C_6F_5 species but provided no unambiguous characterization and are thus neither reported nor analyzed here.

Although FAB-MS analysis was attempted for all complexes, this technique proved unsuccessful for **2**, and the acquired spectra failed to deliver any diagnostic peaks other than for $AuPPh_3^+$. Nevertheless, m/z values that correspond to the cationic complexes are observed for **1**, **3** and **4**. In these spectra, signals attributable to the homoleptic rearrangement product $[Au(PPh_3)_2]^+$ are also present at $m/z = 720$. The molecular ion of **5** was observed but the spectra for **I**–**IV** did not show any unambiguous diagnostic signals that were consistent with the formation of $Au(C_6F_5)$(2-aminoazole) compounds or the products of crystallization.

Molecular structures

The crystal and molecular structures of compounds **1**–**5** and **I**–**IV** were determined by single-crystal X-ray diffraction and are reported for the first time (Figs. 1 – 9). The new compounds consist of: i) either a cationic $[AuPPh_3]^+$ unit (in **1**–**3**) neutralized by a nitrate anion or a AuC_6F_5 fragment (in **5**) coordinated to the endocyclic imine nitrogen of a neutral 2-aminoazole ligand, ii) two $[AuPPh_3]^+$ units, both *S*-coordinated to 2-mercapto-ethyl-cyanamide (**4**), neutralized by a nitrate anion, or iii) $[Au(C_6F_5)_2]^-$ neutralized by various cations (**I**–**IV**), the products of homoleptic rearrangements. For complex **3**, three different crystal structures were obtained, one without any

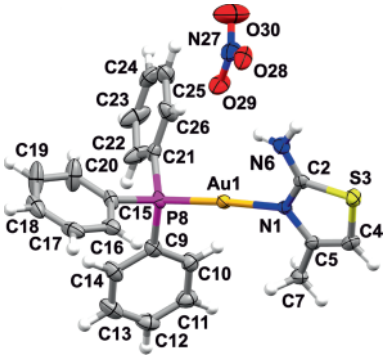

Fig. 1 (color online). Molecular structure of **1** with displacement ellipsoids drawn at the 50 % probability level. Selected bond lengths (Å) and angles (deg): Au1–N1 2.071(3), Au1–P8 2.245(1), N1–C2 1.322(4), N1–C5 1.404(4); N1–Au–P8 175.5(1).

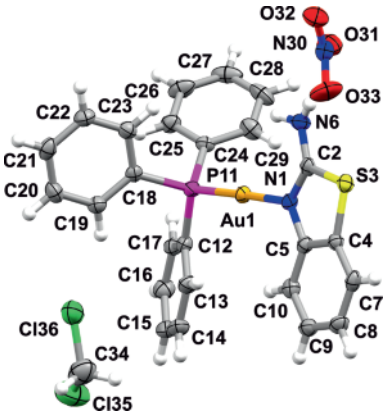

Fig. 2 (color online). Molecular structure of **2** in its CH_2Cl_2 solvate with displacement ellipsoids drawn at the 50 % probability level. Selected bond lengths (Å) and angles (deg): Au1–N1 2.059(3), Au1–P11 2.237(1), N1–C2 1.318(5), N1–C5 1.401(5); N1–Au1–P11 178.3(1).

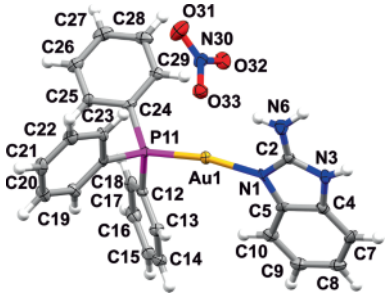

Fig. 3 (color online). Molecular structure of **3a** with displacement ellipsoids drawn at the 50 % probability level. Selected bond lengths (Å) and angles (deg): Au1–N1 2.057(5), Au1–P11 2.234(2), N1–C2 1.325(7), N1–C5 1.389(7); N1–Au–P11 167.3(1).

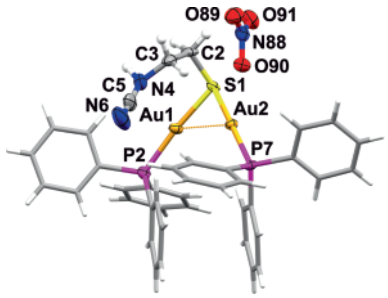

Fig. 4 (color online). Representation of the dinuclear gold(I) complex **4** (one of two crystallographically independent complexes present in the asymmetric unit), with displacement ellipsoids drawn at the 50 % probability level; benzene rings shown as sticks for clarity, intramolecular aurophilic interactions shown as dotted line. Selected bond lengths (Å) and angles (deg) with the corresponding values for the other complex: Au1···Au2 3.114(1)/Au3···Au4 3.090(1), Au1–S1 2.320(3), Au2–S1 2.316(3), Au3–S44 2.325(2), Au4–S44 2.324(3), Au1–P2 2.252(3), Au2–P7 2.258(3), Au3–P69 2.258(2), Au4–P50 2.270(3); S1–Au1–P2 174.7(1), S1–Au2–P7 173.5(1), S44–Au3–P69 175.2(1), S44–Au4–P50 178.5(1).

solvent molecules (**3a)** and two others (**3b**, **3c**) that contain solvent of crystallization. The crystallographic data for the solvates do not contribute much to the further discussion, and their data are reported in the Supporting Information available online (see note at the end of the paper for availability).

The geometry around Au(I) in the two-coordinated Au(I) complexes approaches linearity with L^1–Au–L^2 angles ranging from 167.3(1)° in **3a** to 180.0(4)° in **II**. The distortion of the N–Au–P angle in **3a** is most probably caused by weak interactions of the Au(I) ion with a nitrate ion (Au···O separations of 3.270(4) and 3.306(5) Å). Such interactions are not present in the solvates **3b** and **3c**, with values for the corresponding angles of 177.0(2)° and 178.53(8)°, respectively, and with the nitrate ion located much further from the metal center. The P–Au–S angles [173.5(1)° and 174.7(1)°] in the two complexes of **4**, are slightly less distorted and correspond well to the values reported for similar compounds such as [S(Au_2dppf)] (dppf = 1,1′-bis(diphenylphosphine)ferrocene), 173.8(1)° [34] and [($AuPPh_3$)$_2$(μ-SCH_2CH_2N–CN)], 170.1(1), 176.0(1) and 178.8(1)° [22].

Aurophilic interactions are only present in the dinuclear structure **4** (semi-supported intramolecular in-

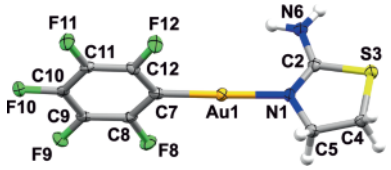

Fig. 5 (color online). Molecular structure of **5** with displacement ellipsoids drawn at the 50 % probability level. Selected bond lengths (Å) and angles (deg): Au1–N1 2.052(4), Au1–C7 1.987(5), N1–C2 1.289(6), N1–C5 1.455(6); N1–Au1–C7 177.5(2).

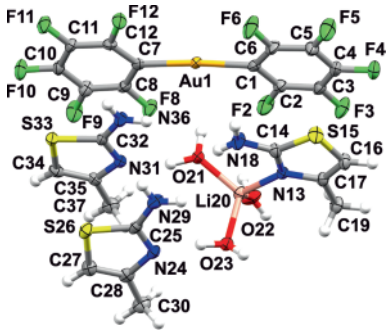

Fig. 6 (color online). Representation of **I** with displacement ellipsoids drawn at the 50 % probability level. Selected bond lengths (Å) and angles (deg): Au1–C1 2.044(3), Au1–C7 2.039(3); C1–Au1–C7 175.5(1).

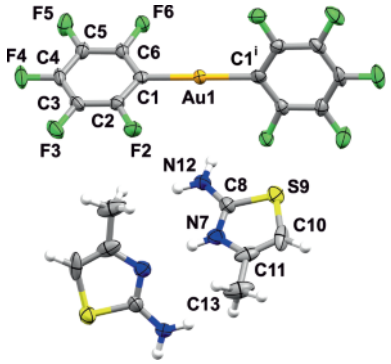

Fig. 7 (color online). Representation of **II** with displacement ellipsoids drawn at the 50 % probability level, asymmetric unit labeled. Selected bond lengths (Å) and angles (deg): Au1–C1 2.044(6); C1–Au1–C1^{i} 180.0(4), where (i): $1-x+1, y, -z+1/2$.

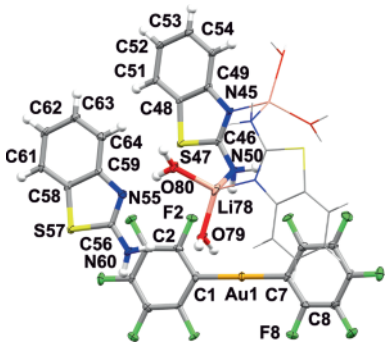

Fig. 8 (color online). Representation of **III** (one of two crystallographically independent moieties present in the asymmetric unit) with displacement ellipsoids drawn at the 50 % probability level; the missing part of the dimeric unit formed during Li^{+} coordination to 2-aminobenzothiazole is shown in wireframe style. Selected bond lengths (Å) and angles (deg): Au1–C1 2.041(5), Au1–C7 2.039(6), Au2–C13 2.033(5), Au2–C19 2.032(5); C1–Au1–C7 178.6(2), C13–Au1–C19 178.1(2).

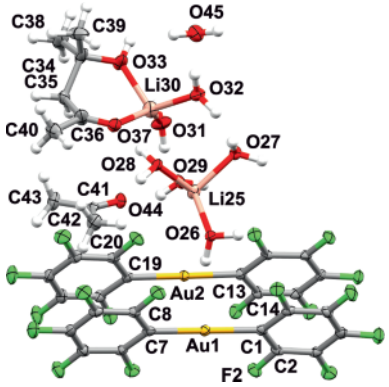

Fig. 9 (color online). Representation of **IV** with displacement ellipsoids drawn at the 50 % probability level; disorder on 4-hydroxy-4-methylpentan-2-one is omitted for clarity. Selected bond lengths (Å) and angles (deg): Au1–C1 2.048(4), Au1–C7 2.043(4), Au2–C31 2.052(4), Au2–C19 2.050(4); C1–Au1–C7 177.6(2), C13–Au2–C19 178.3(1).

teractions) and the structures of **I** and **IV** (intermolecular interactions). The sharp Au–S–Au angle, with values 83.3(1)/84.4(1)° (two crystallographically independent molecules present in the asymmetric unit) in compound **4** facilitates the formation of intramolecular contacts with Au1···Au2 and Au3···Au4 distances of 3.114(1) and 3.090(1) Å, respectively. These values correspond well to those reported for an analogous compound [S(Au$_2$dppf)], Au–S–Au 77.76(1)°, Au···Au 2.882(1) Å [34]. There are no intermolecular aurophilic interactions in **4** but instead, delocalized Au···π(arene) interactions with distances Au1···(C51–C56) 3.71 Å and Au3···(C8–C13) 3.81 Å [35] and weak hydrogen bonds such as N–H···O and C–H···O involving the nitrate ions govern

its solid-state packing. Intermolecular Au···S contacts, Au(2)···S(44) 3.566(3) Å, Au(4)···S(1) 3.358(3) Å, akin to those observed in Au(C_6F_5)(4-methylthiazole-2-thione) (3.529(4) Å) [12] are worth mentioning but, because of the rather long separation, it is hard to estimate their contribution.

The intermolecular aurophilic bonding in **I** and **IV** is facilitated by the nearly co-planar positioning of the two ring systems connected to the gold atoms with the angle between the planes of these rings 4.1° and 2.5°/3.6°, respectively. The anionic complexes linked by interactions between gold atoms form supramolecular centrosymmetric dimers in **I**, with Au···Au = 3.450(1) Å and aggregate into columns in **IV** with Au···Au contacts ranging from 3.489(1) to 3.659(1) Å. A somewhat different situation transpired in the crystal structure of **III**, where despite the co-planarity of the rings (4.06/3.14°), aurophilic contacts are not present. However the hydrogen bond network is abundant, involving many weak C–H···F interactions between perfluorinated benzene rings and the phenyl moieties from 2-aminobenzothiazole.

The preference for the formation of hydrogen bonds over aurophilic associations may well be an enthalpy effect. The energy of an aurophilic interaction (29 – 33 kJ mol^{-1}) has been estimated by NMR experiments to be of the same order of magnitude as a typical hydrogen bond (20 – 30 kJ mol^{-1}) [36]. Calculations by Laguna and co-workers [37] have shown that aurophilic interactions and hydrogen bonds are of comparable strength, and that the competition of these two motifs determines the structural arrangement in the crystal structure of the compounds. The formation of several hydrogen bonds per molecule in the crystal structures whereas the aurophilic bond per molecule ratio would be 1 : 2, therefore results in a much greater gain in energy compared to association *via* aurophilic bonds.

Intermolecular aurophilic interactions in the compounds **1**–**4** are most likely prohibited by the steric demands of the bulky ligands while the orientation of the two rings coordinated to gold in **II** and **5**, with angles between the planes of 66.1° and 82.0°, respectively, could also prohibit the occurrence of short metal contacts.

It is striking that no intermolecular aurophilic interactions occur in the rather simple, complex **5** that is derived from non-bulky ligands, especially considering its remarkable stability in the crystalline form. Once again, hydrogen bonds seem to prevail. In the crystal structure, the neutral molecules are connected by weak hydrogen bonds, involving the amine hydrogen atoms (H6A, H6B) and phenyl fluorine atoms from three adjacent rings, forming supramolecular layers. These are further supported by weak π-π stacking interactions between the phenyl rings (3.512(3) Å with a slippage of 1.228 Å; (symmetry operation $1-x$, $-y$, $-z$) and C–H···π contacts involving the atoms C5–H5A.

Substitution of the nitrate ligand in Au(NO_3)PPh_3 by 2-aminoazole ligands or 2-mercaptoethylcyanamide results in a significant elongation of the Au–P bond from 2.208(3) [38] to 2.245(1) Å in **1** to 2.237(1) Å in **2**, 2.234(2) Å in **3** and 2.252(3) or 2.258(3) Å in **4**. The Au–P bond lengths are similar to those reported for compounds containing imine ligands or S-donor ligands coordinated to $AuPPh_3$ moieties *e. g.* [$AuPPh_3$(ylideneamine)][NO_3] [ylideneamine = 3,4-dimethyl-3*H*-thiazol-2-ylideneamine (2.229(1) Å), 3-methyl-3*H*-benzothiazol-2-ylideneamine (2.225(1) Å) or 1,3-dimethyl-1,3-dihydro-benzimidazol-2-ylideneamine (2.231(1) Å)] [14] as well as [Au{NH=C(NMe_2)$_2$(PPh_3)}]-[CF_3SO_3] and [Au(NH=CPh_2)(PPh_3)][BF_4] (2.229(2) and 2.234(2) Å, respectively) [39] or [S(Au_2dppf)], 2.247(2) Å, [34] and [($AuPPh_3$)$_2$(μ-SCH_2CH_2N-CN)], 2.2757(11) Å [22].

The Au–N bond in the 2-aminoazole ligand in **1**–**3** and **5** seems to be relatively insensitive to changes in the ligand itself or to influences by ligands positioned *trans* thereto. Values vary between 2.071(3) Å (in **1**) and 2.040 (5) Å (in **3b**). These distances are comparable to those reported for examples wherein the gold(I) atom is coordinated to an endocyclic N atom, [Au(C_6F_5)(4-methylthiazole)] 2.081(8) Å [12] and [Au(C_6F_5)(tetrazole)] (tetrazole = 1-methyltetrazole 2.044(3) Å and 1-benzyltetrazole 2.049(4) Å) [13], as well as an exocyclic N atom, [Au(C_6F_5)(ylideneamine)] and [$AuPPh_3$(ylideneamine)][NO_3] [ylideneamine = 3,4-dimethyl-3*H*-thiazol-2-ylideneamine (2.031(4) and 2.036(4) Å), 3-methyl-3*H*-benzothiazol-2-ylideneamine (2.037(5) and 2.028(6) Å) or 1,3-dimethyl-1,3-dihydro-benzimidazol-2-ylideneamine (2.041(5) and 2.040(3) Å)] [14]. Similar Au–N distances have also been reported for the [Au(imine)(PPh_3)]$^+$ complexes [Au(NH=CPh_2)(PPh_3)][BF_4] and [Au{NH=C(NMe_2)$_2$}-(PPh_3)][CF_3SO_3] [2.036(7) Å and 2.044(9) Å, respectively] [39].

The Au–S bonds in compound **4**, Au1–S1 2.319(3) Å/Au2–S1 2.315(3) Å and Au3–S44 2.325(3) Å/Au4–S44 2.324(3) Å, concur with examples in the literature *e. g.* [S(Au_2dppf)], 2.300(2) Å, [34], [($AuPPh_3$)$_2$(μ-SCH_2CH_2N–CN)], 2.3031(10) Å, [22], and other gold compounds with *S*-donor ligands, [Au(C_6F_5)(4-methylthiazole-2-thione)], 2.304(4) Å [12], [Au(C_6F_5)(tht)], 2.317(3) and 2.320(3) Å, [40].

Finally, as far as bond lengths are concerned, the Au–C bond lengths in **I**–**IV** ranging between 2.032(5) – 2.048(4) Å are very similar to those in known gold(I) complexes *e. g.* [Au(C_6F_5)$_2$][Au(pdma)$_2$], (2.062(8) and 2.041(9) Å) [29] and in the reactant [Au(C_6F_5)(tht)], (2.014(9) and 2.03(1) Å) [40], as well as in the S-coordinated [Au(C_6F_5)(4-methylthiazole-2-thione)] (2.057(14) Å) [12], but significantly longer than in the product Au(C_6F_5)(2-aminoazole) (**5**) (1.985(7) Å) or other imine complexes, Au(C_6F_5)ylideneamine [ylideneamine = 3,4-dimethyl-3*H*-thiazol-2-ylideneamine (2.002(5) Å), 3-methyl-3*H*-benzothiazol-2-ylideneamine (2.009(5) Å) or 1,3-dimethyl-1,3-dihydro-benzimidazol-2-ylideneamine (2.009(7) Å)] [14] or [(C_6F_5)Au(4-methylthiazole)] (2.00(1) Å) [12], suggesting that a rather similar electronic influence is exercised by C_6F_5 and S-donor ligands and implying a larger *trans* influence for these two ligands compared to imine ligands.

Crystallization times of several days under non-inert conditions allowed homoleptic rearrangements and the formation of [(C_6F_5)$_2$Au]$^-$ and various cations in the instances of **I**–**IV**. The Li-containing cations of **I**, **III** and **IV** have a distorted tetrahedral geometry around the central Li atom, coordinated to the imine N atom of 2-amino-4-methylthiazole and three water molecules in **I**, to the imine and amine N atoms of adjacent 2-aminobenzothiazole moieties and two water molecules in **III**, and bidentately to two O atoms of 4-hydroxy-4-methylpentan-2-one (resulting from a symmetrical aldol condensation of acetone [41]) and to two water molecules in one cation and to four water molecules in the second cation in **IV**. Lithium chloride that remained from the synthesis of [(C_6F_5)Au(tht)] afforded the formation of the Li^+ cations.

For **II**, an imine atom of the 2-amino-4-methylthiazole ligand has been protonated forming the counter ion, with the said H atom shared with a symmetry-related thiazole unit (symmetry operation: $1-x$, y, $3/2-z$). This entails that the proton sometimes does and sometimes does not occur on the 2-amino-4-methylthiazole molecule (distribution 50/50). The formally single C(sp^2)–N(sp^2) bond, N7–C11, has a length of 1.380(9) Å and the C=N double bond, N7–C8, a length of 1.317(8) Å; both of these values correspond to the respective values in the uncoordinated cationic 2-amino-4-methylthiazolium (1.388(4) and 1.329(3) Å) [42] and uncoordinated 2-amino-4-methylthiazole in **I** (1.396(4) and 1.317(4) Å). The single and double bond character is maintained, indicating little or no delocalization over these bonds.

Hydrogen bonding involving the amine nitrogen atom and either included solvent molecules or the anions, together with C–H···π interactions (the latter ones not present in **3b**) determine the solid-state packing in the [(2-aminoazole)$AuPPh_3$][NO_3] compounds **1**–**3**, further supported by π-π stacking in **2**, **3b** and **3c**.

As mentioned earlier the solid-state structures of **I** and **IV** are defined by a combination of aurophilic interactions between [Au(C_6F_5)$_2$]$^-$ anions and hydrogen bonding involving the ligands of the Li-containing cations, free aminoazole, water and acetone molecules (**IV**), as well as π-π stacking. **II** and **III** on the other hand, are assembled mostly by a very elaborate network of hydrogen bonds, such as N–H···F and C–H···F interactions between the anionic and cationic part of **II**, and N–H···F, N–H···O, O–H···S, O–H···N, O–H···F, and C–H···F interactions between the molecules of **III**.

Conclusion

The first molecular structures of [$AuPPh_3$]$^+$ and AuC_6F_5 units coordinated to 2-aminoazoles were determined and confirmed metal coordination to the softer endocyclic imine rather than the hard exocyclic amine or endocyclic thioether, save intricacies such as an unanticipated 2-aminoazoline ring opening to yield a dinuclear gold(I) coordination compound, μ$_2$-(2-mercapto-ethyl-cyanamide-κ,S)bis(triphenylphosphine)gold(I) nitrate, with short Au···Au contacts which stabilize hypercoordination of the (triphenylphosphine)gold(I) moieties around the anionic S center, or homoleptic rearrangement to generate [Au(C_6F_5)$_2$]$^-$ anions that crystallized with various cations.

Experimental Section

Reactions were carried out under argon using standard Schlenk and vacuum-line techniques. All solvents

were predried on ground KOH or molecular sieves and freshly distilled prior to use. Tetrahydrofuran (THF), *n*-hexane, *n*-pentane and diethyl ether were distilled under N_2 from sodium benzophenone ketyl, acetone from 3 Å molecular sieves, dichloromethane and methanol from CaH_2 and ethanol from magnesium. 2-Amino-4-methylthiazole, 2-aminobenzothiazole and 2-aminothiazoline were purchased from Aldrich and 2-aminobenzimidazole, $AgNO_3$ and KH from Fluka. Literature methods were used to prepare $Au(C_6F_5)$THT [27] from Au(Cl)THT [43], $Au(Cl)PPh_3$ [44] from $HAuCl_4$ [45] and $Au(NO_3)PPh_3$ [25] from $Au(Cl)PPh_3$.

Melting points were determined on a Stuart SMP3 apparatus and are uncorrected. Mass spectra were recorded on an AMD 604 (EI, 70 eV) instrument. NMR spectra were recorded on a Varian 300/400 FT or INOVA 600 MHz spectrometer (^{1}H NMR at 300/400/600 MHz, ^{13}C NMR at 75/100/150 MHz, and ^{31}P NMR at 121/161 MHz) with the chemical shifts reported (in ppm) relative to TMS with the solvent resonance as internal reference or 85 % H_3PO_4 (^{31}P) as external reference. Infrared spectra were recorded on a Thermo Nicolet Avatar 330FT-IR instrument with a Smart OMNI ATR (attenuated total reflectance, Zn-Se) sampler. Elemental analysis was carried out at the School of Chemistry, University of the Witwatersrand. Prior to elemental analysis, products were evacuated under high vacuum for 10 h.

*2-Amino-4-methylthiazole-κN^3-(triphenylphosphine)gold(I) nitrate (**1**)*

The ligand, 2-amino-4-methylthiazole (0.063 g, 0.55 mmol), was added to an equal molar amount (0.29 g, 0.55 mmol) of $Au(NO_3)PPh_3$ in a diethyl ether suspension (60 mL). The resulting colorless snowflake-like suspension was stirred for 1.5 h at room temperature. The formation of the imine coordination complex was accompanied by the formation of a new suspension with a notably different texture and off-white color. The mixture was then stripped of solvent *in vacuo* to yield a colorless solid. The solid was extracted with diethyl ether (50 mL). The solution containing the desired gold(I) complex was filtered through $MgSO_4$ and the filtrate stripped of solvent *in vacuo*. The oily yellow residue was subsequently washed with *n*-pentane (30 mL) to yield the yellow microcrystalline material (0.30 g, 94 %). Single crystals were obtained from a concentrated solution of the product in $(CD_3)_2CO$ in an NMR tube, producing colorless needles at −22 °C. M. p. 94 – 97 °C. – IR (selected bands): ν = 3309, 3172 and 3119 w ($NH_{stretch}$), 1627 s ($NH_{2\ scissor}$), 1583 s (C=C), 1531 s (C=N), 1305 bs (C–N) cm^{-1}. – ^{1}H NMR ($(CD_3)_2CO$): δ = 8.46 (bs, 2H, NH_2), 7.68 (m, 15H, PPh_3), 6.43 (bs, 1H, SCH), 2.40 (s, 3H, CH_3). – ^{13}C NMR ($(CD_3)_2CO$): δ = 189.0 (s, NCS), 155.5 (bs, N*C*C), 136.3 (d, ^2J = 13.2 Hz, *o*-Ph), 133.4 (d, ^4J = 2.8 Hz, *p*-Ph), 130.6 (d, ^3J = 12.2 Hz, *m*-Ph) 129.0 (d, ^1J = 65.0 Hz, *i*-PPh_3), 103.2 (s, S*C*C) 17.8 (s, CH_3). – ^{31}P{^{1}H} NMR ($(CD_3)_2CO$): δ = 30.6 (s, PPh_3). – MS (EI): m/z (%) = 1409 (4), 1032 (4), 721 (28) $[Au(PPh_3)_2]^+$, 571 (4) $[M–NO_3–2H]^+$, 458 (100) $[AuPPh_3–H]^+$, 263 (7) $[PPh_3+H]^+$, 181 (100), 113 (7) $[C_4H_6N_2S–H]^+$. – $C_{22}H_{21}AuN_5O_3PS$ (635.44): calcd. C 41.58, H 3.33, N 11.02; found C 41.22, H 3.21, N 10.98.

*2-Aminobenzothiazole-κN^3-(triphenylphosphine)gold(I) nitrate (**2**)*

Complex **2** was prepared using the same protocol as described above with 2-aminobenzothiazole (0.057 g, 0.38 mmol) and $Au(NO_3)_3PPh_3$ (0.20 g, 0.38 mmol) in diethyl ether (60 mL), yielding a colorless solid (0.19 g, 82 %). Colorless crystals of **2** were obtained from a concentrated solution of the product in CH_2Cl_2 at −22 °C. The unexpected complex, bis(2-aminobenzothiazole)silver(I) nitrate, [46] was obtained from a concentrated solution of the product in acetone at −22 °C. The silver contaminants result from the treatment of $[AuCl(PPh_3)]$ with an excess of $AgNO_3$ to afford the starting material $[AuNO_3(PPh_3)]$. M. p. 97 – 105 °C. – IR (selected bands): ν = 3304, 3170 and 3054 w ($NH_{stretch}$), 1639 s ($NH_{2\ scissor}$), 1542 s (C=C), 1465 s (C=N), 1307 bs (C–N) cm^{-1}. – ^{1}H NMR (CD_2Cl_2): δ = 8.34 (bs, 2H, NH_2), 7.60 (m, 15H, PPh_3), 7.38 and 7.25 (m, 4H, CH). – ^{13}C NMR (CD_2Cl_2): δ = 172.7 (s, NCS), 142.1 (s, N*C*CHCH), 134.5 (d, ^2J = 13.3 Hz, *o*-Ph), 132.8 (bs, *p*-Ph), 130.0 (d, ^3J = 11.0 Hz, *m*-Ph) 129.8 (d, ^1J = 67.4 Hz, *i*-PPh_3), 126.9 (s, NC*C*HCH) 125.2 (s, NCCH*C*H), 124.0 (s, S*C*CHCH), 122.3 (s, SCCH*C*H), 116.7 (s, SC*C*HCH). – MS (EI): m/z (%) = 1409 (3), 1032 (4), 721 (28) $[Au(PPh_3)_2]^+$, 458 (100) $[AuPPh_3–H]^+$, 263 (7) $[PPh_3+H]^+$, 181 (44). – $C_{25}H_{21}AuN_3O_3PS$ (671.47): calcd. C 44.72, H 3.15, N 6.26; found C 45.02, H 3.10, N 6.20.

*2-Aminobenzimidazole-κN^3-(triphenylphosphine)gold(I) nitrate (**3**)*

The same protocol as described above was followed with $Au(NO_3)PPh_3$ (0.090 g, 0.18 mmol) and 2-aminobenzimidazole (0.023 g, 0.18 mmol) to obtain a pure colorless solid (0.103 g, 98 %). Single crystals in the form of colorless needles of **3a** were obtained from slow diffusion of *n*-pentane into an acetone solution of the compound at −22 °C. Crystals of **3b** and **3c** were obtained from concentrated solution of the product in methanol in NMR tubes. M. p. 114 – 116 °C. – IR (selected bands): ν = 3385, 3272 and 3123 w $(NH)_{stretch}$ 1641 m $(NH)_{scissor}$, 1542 m (C=C), 1528 m (C=N), 1312 s (C–N) cm^{-1}. – ^{1}H NMR ($(CD_3)_2CO$): δ = 7.71 (m, 15H, PPh_3), 7.45 (dd, ^3J = 5.9 Hz, ^4J = 3.2 Hz, 2H, NCC*H*), 7.12 (dd, 2H, ^3J = 5.9 Hz, ^4J = 2.9 Hz, NCCH(C*H*)$_2$), 3.19 (bs, 2H, NH_2), NH not observed. – ^{13}C NMR ($(CD_3)_2CO$): δ = 156.9 (s, NCN),

136.2 (d, ^2J = 13.9 Hz, *o*-Ph), 134.3 (d, ^4J = 2.2 Hz, *p*-Ph), 131.5 (d, ^3J = 11.7 Hz, *m*-Ph) 130.2 (d, ^1J = 63.8 Hz, *i*-PPh_3), 133.7 (s, N*C*CHCH), 123.8 (s, NCCH*C*H), 113.9 (s, NC*C*HCH). – ^{31}P NMR ($(CD_3)_2CO$): δ = 33.9 (s, PPh_3). – MS (EI): m/z (%) = 721 (5) $[Au(PPh_3)_2]^+$, 592 (49) $[M–NO_3]^+$, 459 (44) $[AuPPh_3]^+$, 181 (26), 134 (52) $[C_7H_8N_3]^+$. $C_{25}H_{22}AuN_4O_3P$ (654.42): calcd. C 45.87, H 3.39, N 8.56; found C 45.63, H 3.31, N 8.44.

*μ_2-(2-Mercapto-ethyl-cyanamide-κ,S)bis(triphenylphosphine)gold(I) nitrate (**4**)*

Compound **4** was obtained using the experimental procedure as described for **1** with $Au(NO_3)PPh_3$ (0.14 g, 0.26 mmol) and 2-aminothiazoline (0.030 g, 0.26 mmol), yielding a colorless solid as a product (0.10 g, 70 %). Crystals suitable for X-ray diffraction were obtained from a concentrated perdeuterated acetone solution of the product in an NMR tube maintained at −22 °C. M. p. 83 – 87 °C. – IR (selected bands): ν = 3295 w $(NH)_{stretch}$, 2218 w (C≡N), 1663 m $(NH)_{bend}$, 1638 m (C=C), 1618 m (C=N), 1310 s (C–N) cm^{-1}. – ^{1}H NMR ($(CD_3)_2CO$): = δ 7.62 (m, 30H, PPh_3), 4.03 (dd, 2H, ^3J = 7.5 Hz, NCH_2), 3.55 (dd, 2H, ^3J = 7.5 Hz, SCH_2), 2.83 (bs, 1H, NH). – ^{13}C NMR ($(CD_3)_2CO$): δ = 136.1 (d, ^2J = 13.7 Hz, *o*-Ph), 134.2 (d, ^4J = 2.6 Hz, *p*-Ph), 131.5 (d, ^3J = 12.0 Hz, *m*-Ph) 130.4 (d, ^1J = 59.7 Hz, *i*-PPh_3), 171.4 (s, NC), 52.9 (s, NCH_2), 35.0 (s, SCH_2). – ^{31}P NMR ($(CD_3)_2CO$): δ = 37.1 (s, PPh_3). – MS (EI): m/z(%) = 1409 (6), 1019 (45) $[M^+–NO_3+H]^+$, 721 (65) $[Au(PPh_3)_2]^+$, 561 (31) $[M–NO_3–AuPPh_3+H]^+$, 459 (100) $[AuPPh_3]^+$, 280 (15) $[C_3H_5N_2S–NH_2–H+Au]^+$. – $C_{39}H_{35}Au_2N_3O_3P_2S$ (1081.68): calcd. C 43.31, H 3.26, N 3.88; found C 44.01, H 3.20, N 3.63.

*2-Aminothiazoline-κN^3-(pentafluorophenyl)gold(I) (**5**)*

Complex **5** was prepared by adding 2-aminothiazoline (0.056 g, 0.55 mmol) to a solution of $Au(C_6F_5)$THT (0.25 g, 0.55 mmol) in diethyl ether (70 mL) and stirring for 2.5 h. The colorless suspension was then evaporated to dryness *in vacuo*. The colorless residue was extracted with diethyl ether (40 mL) and filtered through $MgSO_4$. The filtrate was reduced *in vacuo* to yield an oily product. The oily product was washed with pentane (10 mL) and dried *in vacuo*. The desired colorless product (0.19 g, 85 %) was isolated. Single crystals of **5** were obtained as colorless blocks from a concentrated solution of the product in deuterated dichloromethane at −22 °C. M. p. 97 – 105 °C [22].

*(2-Amino-4-methylthiazole-κN^3)triaquolithium bis(pentafluorophenyl)aurate(–I) (**I**)*

The ligand, 2-amino-4-methylthiazole (0.199 g, 1.6 mmol), was added to a solution of $[Au(C_6F_5)(tht)]$ (0.468 g, 1.0 mmol) in diethyl ether (50 mL). The resulting yellow suspension was stirred for 2 h. Upon evaporation to dryness *in vacuo* colorless microcrystalline material was obtained. The solid was dissolved in diethyl ether (60 mL) and filtered through $MgSO_4$. With subsequent drying of the filtrate *in vacuo* a colorless product (0.31 g) was obtained. Colorless needles suitable for X-ray diffraction were obtained from a concentrated solution of **I** in CD_2Cl_2 in an NMR tube maintained at −22 °C for 2 days.

*2-Amino-4-methylthiazolium bis(pentafluorophenyl)aurate(–I) (**II**)*

The same protocol as described for the preparation of **I** was used with 2-amino-4-methylthiazole (0.063 g, 0.5 mmol) and $Au(C_6F_5)$THT (0.25 g, 0.55 mmol). The resulting mixture was then stirred for 1.5 h and evaporated to dryness *in vacuo*. The oily residue was washed with three 10 mL portions of pentane and dried *in vacuo* to yield a colorless solid. The product was dissolved in diethyl ether (100 mL). After the addition of a second mol equivalent of $Au(C_6F_5)$THT (0.25 g, 0.55 mmol) to the above solution it was again stirred for 1.5 h and dried *in vacuo*. The colorless product was dissolved in diethyl ether (50 mL) and filtered through $MgSO_4$. The resulting solution was evaporated to dryness yielding a colorless solid (0.23 g). Crystals suitable for X-ray diffraction were obtained from a concentrated solution of the product in CD_2Cl_2 at −22 °C within 4 d.

*(2-Aminobenzothiazole-κN^3)diaquolithium bis(pentafluorophenyl)aurate(–I) (**III**)*

The same experimental procedure as described for compound **I** was used with 2-aminobenzothiazole (0.11 g, 0.49 mmol) and $Au(C_6F_5)$THT (0.22 g, 0.49 mmol), yielding a colorless solid (0.090 g). Colorless needles suitable for X-ray diffraction were obtained from a concentrated solution of **III** in acetone in an NMR tube maintained at −22 °C for several days.

*η^2-(4-Hydroxy-4-methylpentan-2-one-κO^2:κO^4)diaquolithium bis(pentafluorophenyl)aurate(–I) (**IV**)*

The same protocol as described above for compound **I** was used with 2-amino-1-methylbenzimidazole (0.14 g, 0.93 mmol) and $Au(C_6F_5)$(THT) (0.42 g, 0.93 mmol). After evaporation, a beige oily residue was obtained. The oily residue was rinsed with pentane to yield a beige solid (0.56 g). Colorless blocks were obtained by the slow diffusion of *n*-pentane into a concentrated solution of **II** in acetone maintained at −22 °C for a week.

X-Ray diffraction experiments

Crystal data collection and refinement details for compounds **1**–**4** and **5**, **I**–**IV** are summarized in Tables 1

Table 1. Crystal structure data for **1**–**4**.

	1	**2**	**3a**	**4**
Emperical formula	$C_{22}H_{21}AuN_2PS \cdot NO_3 \cdot x$ solvent	$C_{25}H_{21}AuN_2PS \cdot NO_3 \cdot CH_2Cl_2$	$C_{25}H_{22}AuN_3P \cdot NO_3$	$C_{39}H_{35}Au_2N_2P_2S \cdot NO_3$
M_r	635.41	756.37	654.40	1081.63
Crystal shape	needle	needle	block	block
Crystal size, mm^3	$0.09 \times 0.06 \times 0.04$	$0.15 \times 0.08 \times 0.04$	$0.11 \times 0.06 \times 0.05$	$0.13 \times 0.09 \times 0.06$
Temperature, K	100(2)	100(2)	100(2)	100(2)
Crystal system	triclinic	triclinic	monoclinic	monoclinic
Space group	$P\bar{1}$	$P\bar{1}$	$P2_1/c$	$P2_1$
a, Å	9.510(3)	11.052(3)	14.3047(12)	10.4002(12)
b, Å	11.684(4)	11.107(3)	9.5301(8)	26.355(3)
c, Å	12.802(4)	11.719(3)	18.8851(19)	14.1318(16)
α, deg	82.913(5)	105.692(4)	90	90
β, deg	76.729(5)	97.679(4)	116.269(1)	106.677(2)
γ, deg	73.875(5)	90.049(4)	90	90
V, $Å^3$	1327.3(8)	1371.5(5)	2308.6(4)	3710.6(7)
Z	2	2	4	4
$D_{calcd.}$, $g\,cm^{-3}$	1.59	1.83	1.88	1.94
$\mu(MoK_\alpha)$, cm^{-1}	5.7	5.7	6.5	8.1
$F(000)$, e	616	736	1272	2072
hkl range	$-12 \le h \le 11$ $-14 \le k \le 14$ $-16 \le l \le 16$	$-13 \le h \le 13$ $-13 \le k \le 13$ $-14 \le l \le 14$	$-13 \le h \le 17$ $-11 \le k \le 11$ $-23 \le l \le 22$	$-11 \le h \le 12$ $-33 \le k \le 19$ $-17 \le l \le 16$
$((\sin\theta)/\lambda)_{max}$, $Å^{-1}$	0.6315	0.6265	0.6252	0.6271
Refl. measured	14 025	14 750	13 222	21 882
Refl. unique	5501	5576	4706	13 102
R_{int}	0.0236	0.0335	0.0431	0.0357
Param. refined	289	342	313	921
$R(F)/wR(F^2)$[a,b] $[I > 2\,\sigma(I)]$	0.0255/0.0637	0.0279/0.0628	0.0380/0.0801	0.0409/0.0755
$R(F)/wR(F^2)$[a,b] (all refls.)	0.0275/0.0646	0.0319/0.0645	0.0494/0.0847	0.0493/0.0786
GoF (F^2)[c]	1.054	1.043	1.048	1.025
$\Delta\rho_{fin}$ (max/min), e $Å^{-3}$	2.70/−1.17	1.12/−0.75	2.28/−1.39	1.83/−1.09

[a] $R(F) = \Sigma||F_o| - |F_c||/\Sigma|F_o|$; [b] $wR(F^2) = [\Sigma w(F_o^2 - F_c^2)^2/\Sigma w(F_o^2)^2]^{1/2}$, $w = [\sigma^2(F_o^2) + (AP)^2 + BP]^{-1}$, where $P = (\mathrm{Max}(F_o^2, 0) + 2F_c^2)/3$; [c] $\mathrm{GoF} = [\Sigma w(F_o^2 - F_c^2)^2/(n_{obs} - n_{param})]^{1/2}$.

and 2, respectively. The data were collected on a Bruker SMART Apex CCD diffractometer equipped with graphite-monochromatized MoK_α radiation ($\lambda = 0.71073$ Å) [47]. The cell refinement and the data reduction were performed with the software package Bruker SAINT+ [47], and the empirical absorption corrections were performed with SADABS [48]. All the structures were solved using Direct Methods with SHELXS-97 [49, 50] and refined by full-matrix least-squares methods based on F^2 with SHELXL-97 [51, 52]. All non-hydrogen atoms were refined anisotropically. Hydrogen atoms, excluding some coming from -NH, -OH, were positioned geometrically with C–H 0.95 (aromatic), 0.98 (methyl) and 0.99 Å (methylene); N–H 0.88 Å (amine, aromatic) and refined as riding, with $U_{iso}(H) = 1.2\,U_{eq}$ (C, N) and 1.5 U_{eq} (methyl C). The remaining ones were located in a difference map and refined. Restraints were placed on some of the corresponding bond lengths – especially in the case of water molecules. The program MERCURY [53] was used to prepare molecular graphic images.

In the structure of **1**, the solvent molecules could not be assigned because of diffuse electron density. Therefore, the electron density was subtracted, and the SQUEEZE instruction of PLATON was applied [54, 55]. As the crystals were grown from a mixture of solvents, it was difficult to make any assumptions regarding the exact nature of these molecules. Consequently, the tabulated relative molecular mass M_r, $F(000)$, and absorption coefficient (Table 1) are not correct since solvent molecules were not taken into account in these calculations.

The crystal of **4** was found to be a racemic twin, with a contribution of the second component of 37 %. One of the

Table 2. Crystal structure data for **5** and **I**–**IV**.

	5	**I**	**II**	**III**	**IV**
Emperical formula	$C_9H_6AuF_5N_2S$	$C_{12}AuF_{10}\cdot C_4H_{12}LiN_2O_3S\cdot 2(C_4H_6N_2S)$	$C_{12}AuF_{10}\cdot C_8H_{13}N_4S_2$	$C_{14}H_{20}Li_2N_4O_4S_2\cdot 2(C_{12}AuF_{10})\cdot 2(C_7H_6N_2S)$	$2(C_{12}AuF_{10})\ C_6H_{16}LiO_4\cdot H_8LiO_4\cdot C_3H_6O\cdot H_2O$
M_r	466.18	934.58	760.43	1748.91	1376.40
Crystal shape	block	block	needle	block	block
Crystal size, mm^3	$0.09\times0.06\times0.04$	$0.22\times0.20\times0.02$	$0.24\times0.11\times0.03$	$0.27\times0.23\times0.15$	$0.27\times0.20\times0.09$
Temperature, K	100(2)	100(2)	100(2)	100(2)	100(2)
Crystal system	monoclinic	triclinic	monoclinic	triclinic	triclinic
Space group	$P2_1/c$	$P\bar{1}$	$C2/c$	$P\bar{1}$	$P\bar{1}$
a, Å	10.164(3)	8.2753(8)	24.890(6)	9.3133(12)	12.9165(15)
b, Å	9.783(3)	13.8941(13)	7.862(2)	11.8829(16)	13.7196(16)
c, Å	11.455(3)	15.6171(15)	12.595(3)	25.464(3)	15.2175(18)
α, deg	90	115.099(1)	90	103.348(2)	64.202(2)
β, deg	105.455(4)	90.244(2)	110.796(4)	96.384(2)	66.747(2)
γ, deg	90	96.227(2)	90	90.080(2)	62.689(2)
V, $Å^3$	1097.9(5)	1614.0(3)	2304(1)	2723.9(6)	2092.1(4)
Z	4	2	4	2	2
$D_{calcd.}$, $g\,cm^{-3}$	2.82	1.92	2.19	2.13	2.19
$\mu(MoK_\alpha)$, cm^{-1}	13.6	4.8	6.7	5.7	7.1
$F(000)$, e	856	908	1448	1680	1308
hkl range	$-12\le h\le 10$ $-12\le k\le 8$ $-14\le l\le 13$	$-10\le h\le 10$ $-17\le k\le 17$ $-19\le l\le 19$	$-16\le h\le 32$ $-9\le k\le 10$ $-16\le l\le 16$	$-11\le h\le 10$ $-15\le k\le 15$ $-32\le l\le 33$	$-16\le h\le 16$ $-17\le k\le 17$ $-19\le l\le 19$
$((\sin\theta)/\lambda)_{max}$, $Å^{-1}$	0.6263	0.6271	0.6677	0.6638	0.6269
Refl. measured	6207	17 559	7091	17 360	22 673
Refl. unique	2253	6643	2716	12 102	8534
R_{int}	0.0309	0.0280	0.0369	0.0255	0.0269
Param. refined	163	460	169	877	683
$R(F)/wR(F^2)^{a,b}$ $[I>2\,\sigma(I)]$	0.0233/0.0564	0.0263/0.0587	0.0367/0.0879	0.0414/0.1010	0.0233/0.0548
$R(F)/wR(F2)^{a,b}$ (all refsl.)	0.0252/0.0574	0.0299/0.0601	0.0412/0.0899	0.0491/0.1050	0.0280/0.0568
GoF $(F^2)^a$	1.051	1.062	1.072	1.080	1.030
$\Delta\rho_{fin}$ (max/min), e $Å^{-3}$	1.63/−0.59	1.66/−0.89	1.96/−0.85	2.82/−1.19	1.16/−0.93

[a] For definition of R values and GoF, as well as information on the weighting scheme applied, see Table 1.

nitrate ions (N92) was found to be disordered over two positions, with refined site occupancies of 0.67(2) : 0.33(2). As a result, bond length restraints were applied to this anion.

In the structure of **IV**, 4-hydroxy-4-methylpentan-2-one was found to be disordered and modeled into two orientations with refined site occupancies of 0.75(1) : 0.25(1).

CCDC 1018046 – 1018056 contain the supplementary crystallographic data for this paper. These data can be obtained free of charge from The Cambridge Crystallographic Data Centre *via* www.ccdc.cam.ac.uk/data_request/cif.

Supporting information

Supplementary NMR data for the ligands and crystallographic reports for the solvates **3b** and **3c** can be found as Supporting Information (4 pages) available online (DOI: 10.5560/ZNB.2014-4187).

Acknowledgement

We thank the NRF (National Research Foundation, South Africa) and the Alexander von Humboldt foundation (H. G. R.) for financial support.

[1] L. De Luca, *Curr. Med. Chem.* **2006**, *13*, 1 – 23.
[2] E. Buncel, I. Onyido, J. Label, *Compd. Radiopharm.* **2002**, *45*, 291 – 306.
[3] H.-B. Kraatz, N. Metzler-Nolte (Eds.), *Concepts and Models in Bioinorganic Chemistry*, Wiley-VCH, Weinheim, **2006**.

[4] G. Jaouen (Ed.), *Bioorganometallics*, Wiley-VCH, Weinheim, **2006**.

[5] G. Simonneaux (Ed.), *Bioorganometallic Chemistry*, Springer, Berlin, **2006**.

[6] J. M. Matthews, F. E. Loughlin, J. P. Mackay, *Curr. Opin. Struct. Biol.* **2008**, *18*, 484 – 490.

[7] E. R. T. Tiekink, *Inflammopharmacology* **2008**, *16*, 138 – 142, and refs. therein.

[8] S. Nobili, E. Mini, I. Landini, C. Gabbiani, A. Casini, L. Messori, *Med. Res. Rev.* **2010**, *30*, 550 – 580, and refs. therein.

[9] E. Vergara, E. Cerrada, A. Casini, O. Zava, M. Laguna, P. J. Dyson, *Organometallics* **2010**, *29*, 2596 – 2603, and refs. therein.

[10] E. R. T. Tiekink, *Crit. Rev. Oncol./Hematol.* **2002**, *42*, 225 – 248.

[11] J. Zou, P. Taylor, J. Dorman, S. P. Robinson, M. D. Walkinshaw, P. J. Sadler, *Angew. Chem. Int. Ed.* **2000**, *39*, 2931 – 2934.

[12] S. Cronje, H. G. Raubenheimer, H. S. C. Spies, C. Esterhuysen, H. Schmidbaur, A. Schier, G. J. Kruger, *Dalton Trans.* **2003**, 2859 – 2866.

[13] W. F. Gabrielli, S. D. Nogai, M. Nell, S. Cronje, H. G. Raubenheimer, *Polyhedron* **2012**, *34*, 188 – 197.

[14] J. Coetzee, S. Cronje, L. Dobrzańska, H. G. Raubenheimer, M. J. Nell, G. Jooné, H. Hoppe, *Dalton Trans.* **2011**, *40*, 1471 – 1483.

[15] F. Téllez, A. Pena-Hueso, N. Barba-Behrens, R. Contreras, A. Flores-Parra, *Polyhedron* **2006**, *25*, 2363 – 2374, and refs. therein.

[16] N. Metzler-Nolte in *Bioorganometallics*, (Ed.: G. Jaouen), Wiley-VCH, Weinheim, **2006**, pp. 160 – 162.

[17] M. Salmain in *Bioorganometallics*, (Ed.: G. Jaouen), Wiley-VCH, Weinheim, **2006**, pp. 199 – 200.

[18] T. W. Stringfield, R. E. Shepherd, *Inorg. Chem. Commun.* **2001**, *4*, 760 – 765.

[19] T. W. Stringfield, R. E. Shepherd, *Inorg. Chim. Acta* **2003**, *343*, 156 – 168.

[20] J. E. Huheey, E. A. Keiter, R. L. Keiter, *Inorganic Chemistry, Principles of Structure and Reactivity*, 4th ed., Harper Collins College Publishers, New York, **1993**.

[21] L. de Jongh, C. E. Strasser, H. G. Raubenheimer, S. Cronje, *Polyhedron* **2009**, *28*, 3635 – 3641.

[22] M. Bardají, A. Laguna, M. Reyes Pérez, P. G. Jones, *Organometallics* **2002**, *21*, 1877 – 1881.

[23] H. Schmidbaur, *Gold Bull.* **2000**, *33*, 3 – 10.

[24] H. G. Raubenheimer, M. Desmet, G. J. Kruger, *J. Chem. Soc., Dalton Trans.* **1995**, 2067 – 2071.

[25] L. Malatesta, L. Naldini, G. Simonetta, F. Cariati, *Coord. Chem. Rev.* **1966**, *1*, 255 – 262.

[26] L. J. Mathias, D. Burkett, *Tetrahedron Lett.* **1979**, *20*, 4709 – 4712.

[27] R. Usón, A. Laguna, M. Laguna, *Inorg. Synth.* **1989**, *26*, 85 – 87.

[28] W. F. Gabrielli, PhD Dissertation, University of Stellenbosch, Stellenbosch, South Africa, **2005**, pp. 98 – 100 and pp. 159 – 168.

[29] R. Usón, A. Laguna, J. Vicente, J. Garcia, P. G. Jones, G. M. Sheldrick, *J. Chem. Soc., Dalton Trans.* **1981**, 655 – 657.

[30] H. Schottenberger, K. Wurst, U. E. I. Horvath, S. Cronje, J. Lukasser, J. Polin, J. M. McKenzie, H. G. Raubenheimer, *Dalton Trans.* **2003**, 4275 – 4281.

[31] J. Thomas, J. Howarth, K. Hanlon, D. McGuirk, *Tetrahedron Lett.* **2000**, *41*, 413 – 416.

[32] J. Howarth, J. Thomas, K. Hanlon, D. McGuirk, *Synth. Commun.* **2000**, *30*, 1865 – 1878.

[33] R. F. Fenske in *Organometallic Compounds, Synthesis, Structure and Theory*, (Ed.B. L. Shapiro), Texas A &M University Press, College Station, Texas, **1983**, p. 305.

[34] F. Canales, M. C. Gimeno, A. Laguna, P. G. Jones, *J. Am. Chem. Soc.* **1996**, *118*, 4839 – 4845.

[35] I. Caracelli, J. Zuckerman-Schpector, E. R. T. Tiekink, *Gold Bull.* **2013**, *46*, 81 – 89.

[36] H. Schmidbaur, W. Graf, W. Müller, G. Müller, *Angew. Chem., Int. Ed. Engl.* **1988**, *27*, 417 – 419.

[37] A. Codina, E. J. Fernández, P. G. Jones, A. Laguna, J. M. López-de-Luzuriaga, M. Monge, M. E. Olmos, J. Pérez, M. A. Rodriguez, *J. Am. Chem. Soc.* **2002**, *124*, 6781 – 6786.

[38] J. C. Wang, M. N. I. Khan, J. P. Fackler, Jr., *Acta Crystallogr.* **1989**, *C45*, 1008 – 1010.

[39] W. Schneider, A. Bauer, A. Schier, H. Schmidbaur, *Chem. Ber.* **1997**, *130*, 1417 – 1428.

[40] J. Coetzee, W. F. Gabrielli, K. Coetzee, O. Schuster, S. D. Nogai, S. Cronje, H. G. Raubenheimer, *Angew. Chem. Int. Ed.* **2007**, *46*, 2497 – 2500.

[41] W. Nicol, *Chem. Eng. Res. Des.* **2003**, *81*, 1026 – 1032.

[42] V. Fernández, J. C. Doadrio, S. García-Granda, P. Pertierra, *Acta Crystallogr.* **1996**, *C52*, 1412 – 1415.

[43] R. Usòn, A. Laguna in *Organometallic Synthesis*, Vol. 3 (Eds.: R. B. Lang, J. J. Eisch), Elsevier, Amsterdam, **1986**, pp. 324 – 325.

[44] M. I. Bruce, B. K. Nicholson, O. bin Shawkataly, *Inorg. Synth.* **1989**, *26*, 324 – 326.

[45] A. Haas, J. Helmbrecht, U. Nieman in *Handbuch der Präparativen Anorganischen Chemie*, Vol. 2, 3rd ed., (Ed.: G. Brauer), Ferdinand Enke, Stuttgart, **1978**, p. 1014.

[46] C. E. Strasser, L. de Jongh, S. Cronje, H. G. Raubenheimer, *Acta Crystallogr.* **2009**, *E65*, m265–m266.

[47] SMART (version 5.628), SAINT+ (version 6.45), Area Detector Control and Integration Software, Siemens Analytical X-ray Instruments Inc., Madison, Wisconsin (USA) **2002/2003**.

[48] G. M. Sheldrick, SADABS (version 2.03), Program for Empirical Absorption Correction of Area Detector Data, University of Göttingen, Göttingen (Germany) **2002**.
[49] G. M. Sheldrick, SHELXS-97, Program for the Solution of Crystal Structures, University of Göttingen, Göttingen (Germany) **1997**.
[50] G. M. Sheldrick, *Acta Crystallogr.* **1990**, *A46*, 467 – 473.
[51] G. M. Sheldrick, SHELXL-97, Program for the Refinement of Crystal Structures, University of Göttingen, Göttingen (Germany) **1997**.
[52] G. M. Sheldrick, *Acta Crystallogr.* **2008**, *A64*, 112 – 122.
[53] C. F. Macrae, I. J. Bruno, J. A. Chisholm, P. R. Edgington, P. McCabe, E. Pidcock, L. Rodriguez-Monge, R. Taylor, J. van de Streek, P. A. Wood, *J. Appl. Crystallogr.* **2008**, *41*, 466 – 470.
[54] A. L. Spek, PLATON, A Multipurpose Crystallographic Tool, Utrecht University, Utrecht (The Netherlands) **2010**.
[55] A. L. Spek, *Acta Crystallogr.* **2009**, *D65*, 148 – 155.